INT. J. REMOTE SENSING, 20 DECEMBER, 2004,
VOL. 25, NO. 24, 5655–5668

Integration of object-based and pixel-based classification for mapping mangroves with IKONOS imagery

L. WANG

Department of Geography, Texas State University, 601 University Drive, ELA #139, San Marcos, TX 78666, USA; e-mail: lewang@txstate.edu

W. P. SOUSA

Department of Integrative Biology, 3060 VLSB, University of California, Berkeley, CA 94720, USA; e-mail: wpsousa@socrates.berkeley.edu

and P. GONG

Department of Environmental Science, Policy and Management, University of California, Berkeley, CA 94720, USA; e-mail: gong@nature.berkeley.edu

(*Received 26 March 2003; in final form 1 June 2004*)

Abstract. IKONOS 1-m panchromatic and 4-m multispectral images were used to map mangroves in a study site located at Punta Galeta on the Caribbean coast of Panama. We hypothesized that spectral separability among mangrove species would be enhanced by taking the object as the basic spatial unit as opposed to the pixel. Three different classification methods were investigated: maximum likelihood classification (MLC) at the pixel level, nearest neighbour (NN) classification at the object level, and a hybrid classification that integrates the pixel and object-based methods (MLCNN). Specifically for object segmentation, which is the key step in object-based classification, we developed a new method to choose the optimal scale parameter with the aid of Bhattacharya Distance (BD), a well-known index of class separability in traditional pixel-based classification. A comparison of BD values at the pixel level and a series of larger scales not only supported our initial hypothesis, but also helped us to determine an optimal scale at which the segmented objects have the potential to achieve the best classification accuracy. Among the three classification methods, MLCNN achieved the best average accuracy of 91.4%. The merits and restrictions of pixel-based and object-based classification methods are discussed.

1. Introduction

Mangrove forests are highly productive ecosystems that typically dominate the intertidal zone of low energy tropical and subtropical coastlines (Lugo and Snedaker 1974, Kathiresan and Bingham 2001). The constituent species in these forests are often differentially distributed along the intertidal gradient, forming zones of differing species composition with distance from the water's edge. Mangrove habitats and the organisms they support are of significant ecological and economic value. At the same time, their health and persistence are seriously

International Journal of Remote Sensing
ISSN 0143-1161 print/ISSN 1366-5901 online © 2004 Taylor & Francis Ltd
http://www.tandf.co.uk/journals
DOI: 10.1080/014311602331291215

threatened by coastal development projects and various forms of non-renewable exploitation (Saenger *et al*. 1983, Ellison and Farnsworth 1996, Farnsworth and Ellison 1997). Thus, there is an increasing need to monitor and assess mangrove forest structure and dynamics, both to gain a better understanding of their basic biology and to help guide conservation and restoration efforts. The ability to accurately map mangrove species with the tools of remote sensing would greatly assist in this effort.

Although remote sensing has been used to map many of the land cover types on earth, it has not been widely used for mapping mangrove forests. The few studies that have been conducted have concentrated on distinguishing mangrove from non-mangrove habitats, without regard to species of mangrove. Among recent research in this area, Venkataratnam and Thammappa (1993) used Landsat Multispectral Scanner (MSS) data to map mangroves along the coastline of Andhra Pradesh, India. Rasolofoharinoro *et al*. (1998) produced a detailed cartographic inventory of a mangrove ecosystem in Madagascar based on a classification from Satellite pour l'Observation de la Terre (SPOT) images (SPOT 1 and 2). Gao (1998) developed a two-tiered classification scheme based on a SPOT image and applied it to the mangrove mapping in the Waitemata Harbour of Auckland, New Zealand. This method was 81.4% accurate in classifying mangrove versus non-mangrove land cover. Green *et al*. (1998) compared the suitability of three types of data (SPOT XS, Landsat TM, CASI) in mapping mangrove species with five different classification approaches. Gao (1999) conducted a comparative study on mangrove mapping with SPOT XS and Landsat Thematic Mapper (TM) images at 10, 20, 30 m resolution. In general, two conclusions can be drawn from the above studies.

1. Accurate discrimination between mangrove and non-mangrove vegetation was not possible using Landsat MSS and SPOT XS data, while Landsat TM data appeared to be appropriate for this purpose. Due to the small patch size of different mangrove species, they cannot be mapped at a resolution coarser than 30 m.
2. Accurate discrimination among mangrove species was not possible using either type of satellite data, but was possible using images from the Compact Airborne Spectrographic Imager (CASI) airborne sensor.

The successful launch of IKONOS 2 by Space Imaging LLC, has provided higher resolution images of mangrove habitat than previously available, offering the possibility of enhanced discrimination of cover types. This expectation is supported by Mumby and Edwards (2002) finding that IKONOS images allowed significantly higher accuracy than Landsat TM in mapping marine environments. To the best of our knowledge, IKONOS images have not previously been used for mapping mangroves. Therefore, it is worthwhile to evaluate how well one can differentiate mangrove from non-mangrove cover, or distinguish different species of mangrove.

Most traditional classification approaches are based on statistical analysis of individual pixels. These approaches are well-suited to images with relatively coarse spatial resolution. With the availability of Very-High-Resolution (VHR) images, it is anticipated that the classification accuracy of land cover types will improve accordingly. However, the land cover types to be classified usually correspond to a coarser scale. With a finer spatial resolution, the number of detectable sub-class elements increases as well. The resulting increase in the within-class spectral variance may make separation of spectrally mixed land cover types more difficult

(Shaban and Dikshit 2001). Recent research has shown that pixel-based classification methods are not suitable for the VHR image (Scheiewe *et al.* 2001). An alternative solution is to incorporate as much information on spatial neighbourhood properties as possible into the classification process. Object-based classification has been proposed as a means of incorporating such spatial information into the classification procedure. This approach is also consistent with the perspective from the disciplines of geographical or landscape ecology, that it is preferable to work on a meaningful object representing the true spatial pattern rather than a uniform pixel (Blaschke and Strobl 2001). Technically, the object-based methods involve two steps: segmentation and classification. In the segmentation stage, the major task is to partition the whole image into a series of closed objects, which coincide with the actual spatial pattern. Detailed reviews of segmentation methods can be found in Pal and Pal (1993) and Cufi *et al.* (2002).

'Region growing' is among the most commonly used segmentation methods. This procedure starts with the generation of seed points over the whole scene, followed by grouping neighbouring pixels into an object under a specific homogeneity criterion (Kettig and Landgrebe 1976, Lobo 1997, Evans *et al.* 2002). The homogeneity criterion is a measure of local spectral heterogeneity, which is defined with a certain choice of 'spectral closeness' metric (Evans *et al.* 2002). For example, Euclidean distance and Mahalanobis distance are two commonly adopted metrics (Richards 1986, Tilton 1998). The object keeps growing until its spectral closeness metric exceeds a predefined break off value. The higher the break off value, the larger the segmented object will be. In theory, there are unlimited choices of break off value. Thus, for a specific application, it is highly desirable for the user to determine an optimal value automatically. Relating this question back to our mangrove classification, we can solve this problem by finding an optimal break off value so that the resultant objects yield best classification accuracy.

The research reported here is part of a larger investigation (being conducted by W. Sousa) of patterns and mechanisms of mangrove forest regeneration on the Caribbean coast of Panama. The specific goals of this remote sensing study were (i) to evaluate whether IKONOS images can be used to map different cover types in the study area, including mangrove canopies of differing species composition, and (ii) to determine which of three different classification methods provides the best discrimination: pixel-based, object-based, or a hybrid of these methods. We hypothesized the spectral separability among different mangrove canopies would be enhanced by taking the object as the basic unit as opposed to the pixel.

2. Study site and data preparation

2.1. *Study site*

The study was conducted in mainland mangrove forests near the Smithsonian Tropical Research Institute's Galeta Marine Laboratory (9°24′18″ N, 79°51′48.5″ W) at Punta Galeta on the Caribbean coast of Panama, approximately 8 km northeast of the city of Colón.

Three tree species comprise the canopy of the study forests. They are: black mangrove (*Avicennia germinans*), white mangrove (*Laguncularia racemosa*), and red mangrove (*Rhizophora mangle*). Red mangrove forms a pure or nearly pure stand at the seaward fringe. About 10–20 m from the water's edge, white mangrove joins the canopy, forming a nearly even mixture with red mangrove in the low intertidal. In these mixed-species stands, white mangroves reach average heights of 22 m, while red mangroves average 16 to 18 m in height (W. Sousa, unpublished data). So, the crowns of white mangroves tend to be emergent, and therefore more visible in the satellite image than those of red mangroves, which form a lower sub-canopy. Black mangrove joins the canopy in the mid-intertidal, creating a mixed canopy of the three species, and then gradually monopolizes most upper intertidal stands. White mangrove may disappear completely from the canopy in the upper intertidal, or occur only as scattered individuals or small stands (W. Sousa, unpublished data).

2.2. *Data preparation*

Two cloud-free IKONOS images, one panchromatic at 1 m resolution and the other multispectral at 4 m resolution, were acquired on 13 June 2000 at 3:24 pm local time (© 2001, Space Imaging LLC, all rights reserved). The sun elevation was 59.1° and the sun azimuth was 59.6°. The image was radiometrically and geometrically corrected by Space Imaging technicians. With the exclusion of a terrain factor, it was reported that IKONOS Geo products would display a 15 m circular error with 90% confidence (CE90). To obtain a higher accuracy, we carried out another round of geometric correction based on ground control points collected throughout the entire scene. Some of the points were centres of canopy gaps. The rest of the control points were located at distinctive positions along a road and bridge. Field global positioning system (GPS) readings were input to conduct geometric correction. This correction procedure achieved sub-meter accuracy. Pixels in the image are recorded in 11 bits. A 2421×2229 sub-image was extracted from the whole scene to cover our study sites. For the purpose of classification, the 4-m multispectral image was resampled to 1 m and stacked with the 1-m panchromatic image, resulting in a five channel image at a spatial resolution of 1 m.

3. Methods

3.1. *Maximum likelihood classification (MLC) at the pixel level*

Previous research has indicated that maximum likelihood classification is the most effective method in classifying mangroves with traditional satellite remote sensing data (Green *et al.* 1998, Gao 1999). Therefore, we adopted this method as a starting point for our analysis. Since 1988, one of us (W. Sousa) has made regular visits to the study area, mapping a variety of forest features with GPS, and establishing and monitoring permanent plots, transects, and long-term field experiments across the study area. Based on this extensive field experience, a total of seven land cover types were chosen for the classification, including three different types of mangrove canopy, rainforest, gap, lagoon, and road. Since the goal of our study was to evaluate different methods for distinguishing the species composition of mangrove forest canopy in VHR satellite imagery, we focused our efforts on the three most common canopy types in the study area. These are (1) pure red mangrove canopy, typical of fringing stands at the water's edge, (2) low to mid-intertidal, mixed canopy of red and white mangroves with whites usually emergent, as described above, and (3) pure black mangrove canopy typical of many upper intertidal sites. Henceforth, we will refer to these three canopy types by the short-hand titles: red, white, or black canopy. Around the time of image acquisition, a detailed field survey of each representative cover type was conducted. Based on this survey, we delineated a separate set of training and test samples for the purpose of classification.

As stated earlier, we hypothesized that spectral separability among mangrove canopies would be enhanced by taking the object as the basic unit as opposed to the pixel. To test this hypothesis, we began with an exploration of the spectral separability among all seven cover types at the pixel level. We chose Bhattacharya Distance (BD) to measure between-class separability (Richards 1986). Previously, BD was mainly used to select an optimum subset of bands or features for the classification. BD was calculated between two classes at a time by using their means and covariance matrices with the assumption that the two classes are in Gaussian distribution. A high BD value means that two classes are spectrally separable and vice versa. As a result, BD can serve as an indicator to the final performance of the supervised classification. The larger the BD value is, the better the final classification will be. The equation we used to compute BD is described in the PCI user manual (PCI 2001).

3.2. *Object-based classification*

As described in §1, object-based classification began with a segmentation of the whole scene into closed objects. In this study, we applied the segmentation method embedded in eCognition 3.0 software (© Definiens Imaging). This method can be a described as a region merging technique. Details can be found in Baatz and Schape (1999). Briefly, this method generates a sequence of seed points from a dither matrix produced by a binary counter. Then starting from each seed point, at each step, a pair of neighbouring image objects will be merged into one large object. The merging decision is made with local homogeneity criteria. The homogeneity criteria are defined by equation (1):

$$f = \sum_{i=1}^{i=n} Wi\left(n_{Merge}\sigma_{Merge} - \left(n_{Obj1}\sigma_{Obj1} + n_{Obj2}\sigma_{Obj2}\right)\right) \quad (1)$$

where n is the number of bands and W_i is the weight for the current band, n_{Merge}, n_{Obj1} and n_{Obj2} are respectively the number of pixels within merged object, initial object 1, and initial object 2. σ_{Merge}, σ_{Obj1}, σ_{Obj2} are the variances of merged object, initial object 1, and initial object 2. f is the derived local tone heterogeneity weighted by the size of image objects and summed over n image bands. In this study, an equal weight value (one) was assigned to all the Wi.

To stop the merging procedure, f must exceed a break off value, which has to be determined beforehand. A small break off value will give rise to a small object size on average, while a large break off value will lead to a big object size on average. Due to this property, the break off value is termed as 'scale parameter' in the context of this method. As a result, the scale parameter is an abstract value that determines the maximum possible change of heterogeneity caused by fusing several objects.

In principle, there are unlimited choices of scale parameters. The final decision of scale parameter is often made by an interpreter based on his or her visual inspection of the image, rather than quantitative criteria. Nevertheless, in the classification situation, it is very hard for the interpreter to tell at which scale parameter the classification accuracy is maximized. It is also very time consuming to conduct classification with all the possible scale parameters. Therefore, we developed a method to choose the optimal scale parameter specific to our mangrove canopy classification purposes. This method is described in the following section.

3.3. *A new method to choose an optimal scale parameter in segmenting homogeneous objects*

BD has mainly been used in analysing class separability to aid selection of optimum bands. However, in this study, we decided to apply this measure in searching for the optimal scale parameter. To be consistent, we preserved the same set of training samples used in the maximum likelihood classification. Taking the training samples as masks, we derived a new image on which training pixels still kept their spectral information while other pixels were assigned a zero value. Then we segmented the new image at various candidate scale parameters with the method introduced in §3.2. At this stage, each object becomes the basic training unit rather than an individual pixel, and correspondingly, the mean grey value of each object was calculated to represent this object's spectral information. Based on these mean spectral values, we derived the pair-wise BD among seven covers at each scale. As a result, the scale at which the BD reaches its maximum was considered the optimal scale and therefore used in the segmentation for the whole scene.

3.4. *Nearest-neighbour (NN) classification at object level*

For the image objects obtained through segmentation at the optimal scale, we applied the nearest neighbour classifier based on the same set of training samples that were applied in MLC. As a result, each object was assigned to one of the seven cover types. The nearest neighbour classifier functions in the following fashion. First, a feature space was defined (i.e. in this study, the five image channels constitute a five-dimensional feature space) in which each image object becomes a point. Since the training samples of each class occupy a spatially clustered location, the final assignment of an object will go to the class that has the sample nearest to the object in the given feature space. In this manner, a thematic map was generated and classification accuracy using pixels as the spatial unit was compared to that using maximum likelihood classification on the same test set.

3.5. *Integrating pixel and object-based (MLCNN) methods*

Based on our experience with MLC and NN, we hypothesized that the combination of a pixel and object-based method would achieve the best classification accuracy in this mangrove study. To test this hypothesis, we designed an integrated classification scheme. With the analysis of the spectral separability conducted at the pixel and object levels, we first performed maximum likelihood classification at the pixel level by merging the spectrally inseparable classes to one class. Those classes with good separability were then masked out and only spectrally mixed classes were further investigated with the object-based classification. If our hypothesis is true, i.e. that the spectral separability among mangrove canopies will be enhanced at a certain object level, then we can expect to achieve a more accurate classification among these mixed classes with the object-based classification. To evaluate this hypothesis, we combined the two classification results at the pixel and object level to produce the final thematic map.

4. Results

4.1. *Spectral separability*

Theoretically, BD ranges from a minimum of 0 to a maximum of 2. A rule of thumb for interpreting a BD value is as follows. A BD value less than 1 indicates a very poor separability while a BD value less than 1.9 and larger than 1 indicates

Table 1. Bhattacharya Distance at the pixel level.

Category	1	2	3	4	5	6	7
1. Red canopy	0						
2. Black canopy	0.66	0					
3. White canopy	1.91	1.74	0				
4. Gap	1.81	1.57	1.77	0			
5. Lagoon	2.00	2.00	2.00	1.94	0		
6. Rainforest	0.80	1.27	1.92	1.83	2.00	0	
7. Road	1.03	1.04	1.24	1.00	1.97	0.71	0

that two classes can be separable to some extent. Only when the BD value is larger than 1.9 can we say a very good separability exists between two classes (PCI 2001). Table 1 lists the pairwise BD calculated from training samples at the pixel level. Previous experience indicates that it is difficult to distinguish rainforest vegetation from the fringing coastal mangroves using Landsat MSS and aerial photography (Kay *et al.* 1991). Our exploration confirms this difficulty. BD between rainforests and red mangrove canopy equals 0.8 and BD between rainforests and black mangrove canopy equals 1.27. An even poorer spectral separability (BD = 0.66) was found between red mangrove and black mangrove canopies. White mangrove canopy, gap, and lagoon exhibit a good degree of separation from other classes. Although road has a poor separability with the three mangrove canopy types and rainforests, it is not a concern for this specific application. Consequently, when we began to select training samples for the classification, we tended to choose more training samples from red mangrove canopy, black mangrove canopy, and rainforest as a strategy to compensate for their poor separability.

We used the method described in §3.2 and §3.3 to explore the object-level spectral separability of the seven cover classes at different spatial scales, segmenting the image at scale parameters of 1, 5, 10, 15, 20, and 25. There are two reasons why we did not explore a scale value over 25. First, when a scale parameter exceeds 25, the generated object size in red mangrove canopy tends to become larger than what was observed in the field. Second, with the same set of training samples, scale value over 25 left an insufficient number of objects to use in the BD calculation. When the scale parameter is 1, the average object size is 1.5, which means each derived object only contains 1.5 pixels. We examined objects generated at this scale and found they were very similar to the original pixel level, thus, we used the BD calculated at the pixel-level from the original image for the spectral separation at this scale. For the other five scales, we calculated a separate set of the BD using the mean spectral values of objects generated at each scale (table 2).

Our object-level analysis focused on the three pairs of land cover types that proved to be the most difficult to separate at the pixel scale: red mangrove versus black mangrove canopies, red mangrove canopy versus rainforests, as well as black mangrove canopy versus rainforests. Figure 1 illustrates that other than scales 5 and 10, where BD value is lower than that at the pixel level scales 15, 20, 25 shows a steady increase of BD value for all three pairs of classes and they all outperform the BD value at the pixel level. This result supported our hypothesis that the spectral separability among some mangrove species canopies is enhanced at a certain object level.

Table 2. Bhattacharya Distance at different scales.

(*a*) Scale parameter = 5.

Category	1	2	3	4	5	6	7
1. Red canopy	0						
2. Black canopy	0.59	0					
3. White canopy	1.85	1.63	0				
4. Gap	1.64	1.41	1.54	0			
5. Lagoon	2.00	2.00	2.00	1.98	0		
6. Rainforest	0.75	1.24	1.89	1.75	2.00	0	
7. Road	1.98	1.99	1.85	1.96	2.00	1.91	0

(*b*) Scale parameter = 10.

Category	1	2	3	4	5	6	7
1. Red canopy	0						
2. Black canopy	0.61	0					
3. White canopy	1.87	1.73	0				
4. Gap	2.00	2.00	2.00	0			
5. Lagoon	2.00	2.00	2.00	2.00	0		
6. Rainforest	0.80	1.24	1.92	2.00	2.00	0	
7. Road	1.99	2.00	1.89	2.00	2.00	1.94	0

(*c*) Scale parameter = 15.

Category	1	2	3	4	5	6	7
1. Red canopy	0						
2. Black canopy	0.66	0.00					
3. White canopy	1.90	1.70	0.00				
4. Gap	1.71	1.44	1.66	0.00			
5. Lagoon	2.00	2.00	2.00	1.98	0.00		
6. Rainforest	0.86	1.24	1.93	1.74	2.00	0.00	
7. Road	2.00	2.00	1.92	1.97	2.00	1.96	0

(*d*) Scale parameter = 20.

Category	1	2	3	4	5	6	7
1. Red canopy	0						
2. Black canopy	0.82	0					
3. White canopy	1.94	1.81	0				
4. Gap	1.74	1.48	1.77	0			
5. Lagoon	2.00	2.00	2.00	1.98	0		
6. Rainforest	0.88	1.28	1.95	1.73	2.00	0	
7. Road	2.00	2.00	1.97	1.99	2.00	1.99	0

(*e*) Scale parameter = 25.

Category	1	2	3	4	5	6	7
1. Red canopy	0						
2. Black canopy	1.04	0	1.90	1.58	2.00	1.35	
3. White canopy	1.97	1.90	0	1.85	2.00	1.97	
4. Gap	1.79	1.58	1.85	0	1.98	1.75	
5. Lagoon	2.00	2.00	2.00	1.98	0	2.00	
6. Rainforest	1.00	1.35	1.97	1.75	2.00	0	
7. Road	2.00	2.00	1.98	1.97	2.00	1.99	0

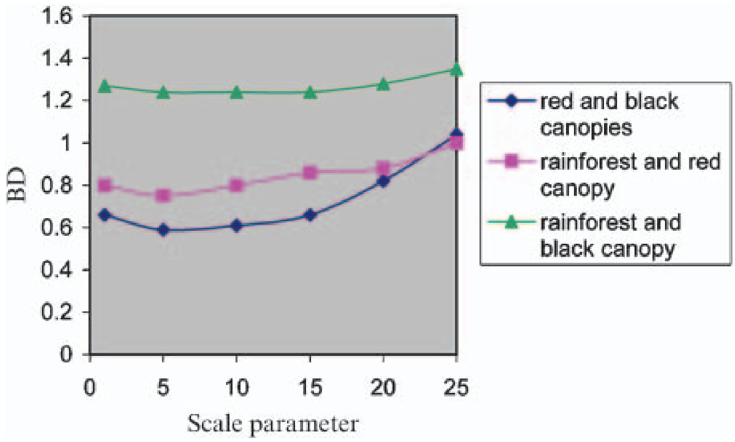

Figure 1. Changes of three pairwise BD values over six scale parameters.

4.2. *Classification accuracy*

Classification accuracy was separately assessed based on the same testing set for the three classification methods; the error matrices are presented in tables 3–5.

MLC yields an average accuracy of 88.9% over the seven cover types (table 3). Consistent with the prediction of spectral separability, red mangrove canopy was classified with the lowest accuracy, only 71.3%. Classification accuracy is also modest for black mangrove canopy and rainforests with an average accuracy value of 81.8% and 81.0% respectively.

NN produces a high κ value (0.94) although with a lower average accuracy (80.4%) compared to that of MLC (table 4). This is because the three cover types that were poorly classified by MLC (red mangrove canopy, black mangrove canopy, and rainforest) all increased in classification accuracy. The accuracy for red mangrove canopy increased from 71.3% in MLC to 77.5% in NN. Black mangrove canopy classification gained an additional 8% accuracy with NN over that with MLC. Rainforest performed even better, improving from 81% to 100%. Given the larger training samples in these three classes compared with other classes, the κ value increased by 0.21. However, the drop in the average accuracy is due to a sharp decrease in accuracy for white mangrove canopy from 97.9% to 21.9%. Fifty-seven per cent of pixels classified as white mangrove canopy from NN are actually rainforest and 21.1% are black mangrove canopy, according to the reference. This low accuracy can be partly attributed to the relatively smaller number of samples of white mangrove canopy compared with that of black mangrove and rainforest. We also conducted a visual inspection of the segmented objects. We paid special attention to the transition of the two different cover types because if the segmented object contains pixels from two different cover types, there is no other way to correct this error, given a single object has become the basic unit, and thus, undividable. Our results did show that in the fringe of red mangroves and in the white mangrove canopy there are some incorrectly segmented objects, which were actually mixed objects containing pixels from both cover types. The classification of these mixed objects caused an error in the edge of two cover types.

With MLCNN, we derived the highest average accuracy (91.4%) among the three methods. This is because white mangrove canopy, gap, lagoon and road

Table 3. Error matrix of maximum likelihood classification at the pixel level ($\kappa = 0.730$).

Category	1	2	3	4	5	6	7	Sum accuracy (%)
1. Red canopy	71.3	18.5	0.5	0.1	0	9.7	0	71
2. Black canopy	13.3	81.8	0.2	1.1	0	3.6	0	82
3. White canopy	0	0.8	97.9	0	0	1.2	0	98
4. Gap	0.7	2.6	0	95.2	0.7	0.7	0	95
5. Lagoon	0	0	0	3.9	96.1	0	0	96
6. Rainforest	14.1	3.4	0.7	0.8	0	81	0	81
7. Road	0	0	1.3	0	0	0	98.7	99
Accuracy (%)	72	76	97	94	99	84	100	88.9

Table 4. Error matrix of nearest neighbour classification at the object (scale = 25) level ($\kappa = 0.94$).

Category	1	2	3	4	5	6	7	Sum accuracy (%)
1. Red canopy	77.5	11.6	0	0	0	10.9	0	78
2. Black canopy	3.1	89.8	0	0	0	7.2	0	90
3. White canopy	0	21.1	21.9	0	0	57	0	22
4. Gap	0	22.7	0	76.6	0	0.7	0	77
5. Lagoon	0	0	0	2.9	97.1	0	0	97
6. Rainforest	0	0	0	0	0	100	0	100
7. Road	0	0	0	0	0	0	100	100
Accuracy (%)	96	62	100	96	100	57	100	80.4

Table 5. Error matrix of integrated classification ($\kappa = 0.81$).

Category	1	2	3	4	5	6	7	Sum accuracy (%)
1. Red canopy	73.7	7.7	0.5	0.1	0	18	0	74
2. Black canopy	2.2	92.4	0.2	1.1	0	4.1	0	92
3. White canopy	0.8	0	97.9	0	0	1.2	0	98
4. Gap	0.7	3	0	94.8	0.7	0.7	0	95
5. Lagoon	0	0	0	3.9	96.1	0	0	96
6. Rainforest	6.5	5.5	0.7	0.8	0	86.4	0	86
7. Road	0	0	1.3	0	0	0	98.7	99
Accuracy (%)	88	85	97	94	99	78	100	91.4

retained the high accuracy achieved with MLC, while red and black mangrove canopies benefited from the NN method. The accuracy for rainforest went up from 81% to 86.4%. This is because rainforest has some portions of spectral overlap with red and black mangrove canopies, while the merged class based on red and black mangrove canopies produced a better spectral separation with rainforest. The relatively lower κ value for MLCNN compared with NN was caused by the decreasing accuracy of rainforests, which had larger training samples as opposed to other classes. Figure 2 provides a graphic comparison of the classification accuracy with the three methods for each cover type. Figure 3 provides the classification map with MLCNN.

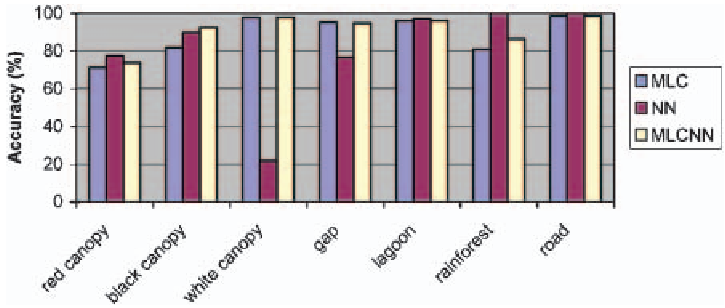

Figure 2. Comparison of classification accuracy for each cover type.

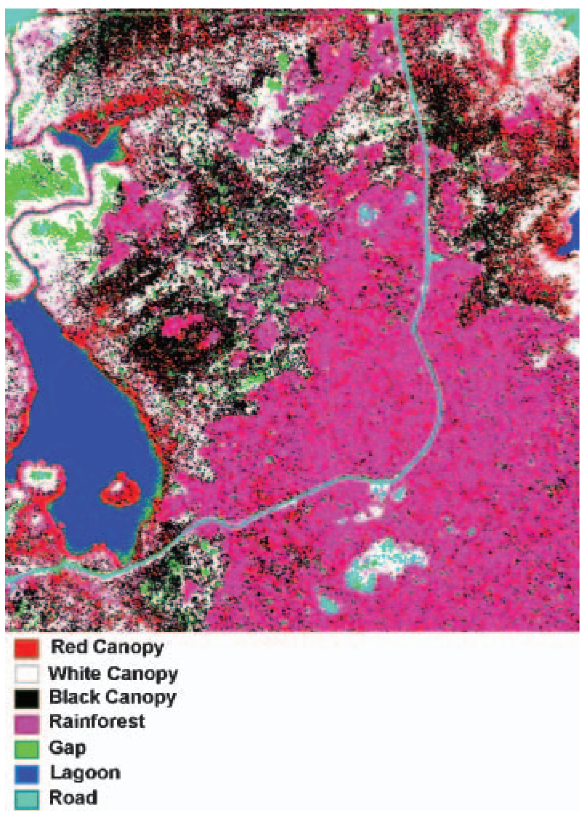

Figure 3. Classification with MLCNN.

5. Discussion

Segmentation is critical to object-based classification. Usually, the user has to decide the specific scale at which to segment an image into objects. However, this search process can be very subjective because it is highly dependent on the interpreter's experience. We used the BD as a quantitative index to guide us in choosing the optimal scale parameter for segmentation. Using this index, we confirmed our hypothesis that spectral separability between some mangrove species canopies can be enhanced at a certain object level as opposed to the pixel level. Second, we used the index as a means of choosing the optimal scale parameter among all possible values. The optimal scale was defined as that which maximized BD. This approach should make object-based classification more efficient and effective.

We found that there were advantages and disadvantages to both the pixel and object-based methods. The pixel-based method retains the rich spectral information contained in the original image and has the finest spatial scale (1 m in this study), but this fine spatial scale does not result in a good differentiation between red mangrove and black mangrove canopies. On the other hand, the object-based method generalizes the spectral information in a spatial neighbour, defined by the local homogeneity criterion. This generalization exaggerates the spectral distinction between spectrally mixed classes, and therefore improves the efficiency of classification. Nevertheless, this generalization also has the risk of incorporating pixels from different classes into one object. Since the object is the smallest unit in the subsequent classification process, the classification accuracy would be decreased. With the segmentation method used in this study, we found it is impossible to ensure that every object derived from the homogeneity criteria contained only one class of pixels. This mixed-object effect will get even worse along the edge or borders of two cover types. Therefore, we adopted an integration of the pixel and object-based methods. In this way, only two difficult-to-separate covers (red mangrove and black mangrove canopies) were input to the object-based method while other cover types were resolved with the pixel-based classification. Since at our study sites, pure stands of red mangrove and black mangrove are spatially separated by a white mangrove canopy (i.e. mixed red/white stands with a largely white overstory) and not directly connected in most places, the mixed-object effect at the edge is largely minimized.

One drawback of our method relates to the selection of training samples. One must use polygons of a relatively large size so that in examining the BD at different scales there will be a sufficient number of objects to serve as training samples.

There is a growing consensus in the field of remote sensing that classification with IKONOS image should use as much spatial information as possible. The region merging segmentation used in this study can be treated as one way to integrate spatial information in the classification. There are still other possible ways to incorporate spatial information, for example, texture and contextual methods. In this study, we did not apply these methods. It will be very valuable to investigate their contribution in the classification of our study site. A comparison of various methods incorporating spatial information will provide guidance in selecting appropriate methods for many other applications.

Mangrove forests provide a number of important ecosystem services including protection from storm surge, trapping of sediment and pollutants in terrestrial runoff, and serving as nursery habitat for numerous commercially important species of fish and crustaceans. These forests are increasingly threatened by coastal development, destructive forms of resource extraction, and sea-level rise associated with climate change. Many mangrove forests cannot be easily accessed for regular on-site monitoring, so the ability to remotely detect and map changes in the cover of different mangrove forest types is critical to management efforts. Mapping mangrove species distributions using conventional remote sensing imagery has proven very challenging due to the low spatial resolution and absence of spectral discrimination. With the emergence of VHR satellite imagery, it was expected that species-level discrimination and mapping would be possible. However, to date, very few studies have critically evaluated this potential use of VHR imagery in any habitat. To our knowledge, ours is the first study to examine this question in mangrove systems. Mumby and Edwards (2002) evaluated the ability of IKONOS imagery to discriminate tropical marine environments (reefs and seagrass beds) in the Turks and Caicos Islands (British Virgin Islands). They found that habitats could be discriminated at a coarse scale (reef versus seagrass), but not at the finer scale of species-assemblages within a habitat. In this paper, we report a method for effectively discriminating different assemblages of mangrove species from IKONOS imagery. Specifically, we demonstrate that an integrated pixel- and object-based classification of IKONOS imagery can provide a valuable tool for mapping mangrove forest species composition, a capability that should be a great value to resource managers.

6. Conclusions

A new method to choose an optimal scale parameter in segmentation, with the criterion that Bhattacharya Distance is maximized, has been proposed and applied to a defined region-merging segmentation. Three classification methods: MLC, NN and MLCNN were applied to the mapping of three different mangrove canopy types and four other cover types at our study sites on the Caribbean coast of Panama. Results indicate IKONOS images can be used to map mangroves canopies and non-mangrove cover in our study sites with an average accuracy of 91.4% using the MLCNN method. At the optimal scale, the classification of two spectrally mixed classes, red mangrove and black mangrove canopies, was improved by object-based classification compared to pixel-based classification. The integrated classification method MLCNN outperformed the other two methods (MLC and NN) in this study. Further evaluation is required to demonstrate that our method gives a consistent result at other study sites.

Acknowledgments

We thank two anonymous reviewers for their instructive comments on the manuscript. The study was supported by grants to W. Sousa from the National Science Foundation (DEB-9221074, DEB-9615887 and DEB-0108146), the University of California, Berkeley Committee for Research, the University of California, Berkeley College of Letters and Sciences Faculty Research Fund for the Biological Sciences, and the Miller Institute for Basic Research in Science. We are grateful to the many undergraduate and graduate student field assistants who helped with the sampling studies that ground-truthed our image analysis.

We thank the Smithsonian Tropical Research Institute for excellent logistical support and for allowing us to use the Galeta Marine Laboratory. The field portion of the project was conducted under research permits from Panama's Instituto Nacional de Recursos Naturales Renovables and Autoridad Nacional del Ambiente. We especially thank the Republic of Panama for preserving their forests and making them available for study.

References

BAATZ, M., and SCHAPE, A., 1999, Object-oriented and multi-scale image analysis in semantic networks. *Proceedings of the 2nd International Symposium on Operationalization of Remote Sensing, 16–20 August 1999* (Enschede, The Netherlands: ITC).

Blaschke, T., and Strobl, J., 2001, What's wrong with pixels? Some recent developments interfacing remote sensing and GIS. *GeoBIT/GIS*, **6**, 12–17.

Cufi, X., Munoz, X., Freixenet, J., and Marti, J., 2002, A review of image segmentation techniques integrating region and boundary information. *Advances in Imaging and Electron Physics*, **120**, 1–39.

Ellison, A. M., and Farnsworth, E. J., 1996, Anthropogenic disturbance of Caribbean mangrove ecosystems: past impacts, present trends, and future predictions. *Biotropica*, **4**, 549–565.

Evans, C., Jones, R., Svalbe, I., and Berman, M., 2002, Segmenting Multispectral Landsat TM images into field units. *IEEE Transactions on Geoscience and Remote Sensing*, **5**, 1054–1064.

Farnsworth, E. J., and Ellison, A. M., 1997, The global conservation status of mangroves. *Ambio*, **6**, 328–334.

Gao, J., 1998, A hybrid method toward accurate mapping of mangroves in a marginal habitat from SPOT Multispectral data. *International Journal of Remote Sensing*, **10**, 1887–1899.

Gao, J., 1999, A comparative study on spatial and spectral resolutions of satellite data in mapping mangrove forests. *International Journal of Remote Sensing*, **14**, 2823–2833.

Green, E. P., Clark, C. D., Mumby, P. J., Edwards, A. J., and Ellis, A. C., 1998, Remote sensing techniques for mangrove mapping. *International Journal of Remote Sensing*, **5**, 935–956.

Kathiresan, K., and Bingham, B. L., 2001, Biology of mangroves and mangrove ecosystems. *Advances in Marine Biology*, **40**, 81–251.

Kay, R. J., Hick, P. T., and Houghton, H. J., 1991, Remote Sensing of Kimberley rainforests. In *Kimberley Rainforests*, edited by N. L. McKenzie, R. B. Johnston, and P. O. Kendrick (Chipping Norton: Surrey Beatty and Sons), pp. 41–51.

Kettig, R. L., and Landgrebe, D. A., 1976, Classification of multispectral image data by extraction and classification of homogeneous objects. *IEEE Transactions on Geoscience and Remote Sensing*, **1**, 19–26.

Lobo, A., 1997, Image segmentation and discriminant analysis for the identification of land cover units in ecology. *IEEE Transactions on Geoscience and Remote Sensing*, **5**, 1136–1145.

Lugo, A. E., and Snedaker, S. C., 1974, The ecology of mangroves. *Annual Review of Ecology and Systematics*, **5**, 39–64.

Mumby, P. J., and Edwards, A. J., 2002, Mapping marine environments with IKONOS imagery: enhanced spatial resolution can deliver greater thematic accuracy. *Remote Sensing of Environment*, **2–3**, 248–257.

Pal, N. R., and Pal, S. K., 1993, A review on image segmentation techniques. *Pattern Recognition*, **9**, 1277–1294.

PCI, 2001, PCI Geomatics 8.2 User Manual, Part: signature separability, Ontario, Canada, http://www.Pcigeomatics.com/.

Rasolofoharinoro, M., Blasco, F., Bellan, M. F., Aizpuru, M., Gauquelin, T., and Denis, J., 1998, A remote sensing based methodology for mangrove studies in Madagascar. *International Journal of Remote Sensing*, **10**, 1873–1886.

Richards, J. A., 1986, *Remote Sensing Digital Image Analysis: An introduction* (Berlin: Springer-Verlag).

Saenger, P., Hegerl, E., and Davis, J., 1983, Global status of mangrove ecosystems. *The Environmentalist*, **3**, 1–88.

Scheiewe, J., Tufte, L., and Ehlers, M., 2001, Potential and problems of multi-scale segmentation methods in remote sensing. *GeoBIT/GIS*, **6**, 34–39.

Shaban, M. A., and Dikshit, O., 2001, Improvement of classification in urban areas by the use of textural features: the case study of Lucknow City, Uttar Pradesh. *International Journal of Remote Sensing*, **4**, 565–593.

Tilton, J. C., 1998, Image segmentation by region growing and spectral clustering with a natural convergence criterion. *Proceedings of the 1998 International Geoscience Remote Sensing Symposium (IGARSS'98), 6–10 July 1998* (Seattle, WA), pp. 1766–1768.

Venkataratnam, L., and Thammappa, S. S., 1993, Mapping and monitoring areas under prawn farming. *Interface: A Bulletin from the NRSA Data Centre*, **4**, 4–7.